Available online at www.journalijmrr.com

INTERNATIONAL JOURNAL OF MODERN RESEARCH AND REVIEWS

ISSN: 2347-8314

Int. J. Modn. Res. Revs.
Volume 2, Issue 12, pp 558-565, December, 2014

ORIGINAL ARTICLE

THE INFLUENCE OF Hg(II) DOPING ON THE PROPERTIES OF AMMONIUM DIHYDROGEN PHOSPHATE CRYSTALS

P. Punitha and *S. Senthilkumar

Chemistry Wing (DDE), Annamalai University, Annamalainagar 608 002, India

Article History: *Received 15th October,2014, Accepted December 29th 2014, Published 31st December,2014*

ABSTRACT

The influence of transition metal (Hg) at various concentrations (1, 5 and 10 mol%) doping on the properties of ammonium dihydrogen phosphate (ADP) were grown from aqueous solutions by slow evaporation techniques. The grown crystals were characterized by FT-IR, UV-Vis absorption spectroscopy, powder X-ray diffraction (XRD), thermogravimetric and differential thermal analysis (TGA-DTA), scanning electron microscopy-energy dispersive spectroscopy (SEM-EDS) and nonlinear optical (NLO) analysis. FT-IR studies confirm the functional groups of the crystal. UV-Vis study shows that the transparency is not affected much by the dopants. Crystal structure has been studied by powder X-ray diffractions. Pure and doped crystals both possessed tetragonal structure. The thermogravimetric analysis reveals the purity of the sample and no decomposition is observed up to the melting point. SEM photograph exhibit the effectiveness of the impurity is changing the surface morphology of ADP doped crystals. The second harmonic generation (SHG) efficiency is enhanced greatly when the concentration of dopants is low and the efficiency is not much pronounced in the case of high concentration.

Keywords: Crystal growth, X-ray diffraction, Spectral analysis, Thermal analysis, Nonlinear optical materials.

1.INDRODUCTION

Ammonium dihydrogen phosphate (ADP) is an interesting material with varied application as a piezoelectric material in transducer devices, nonlinear optics (NLO), electro optics and as monochromatic for X-ray fluorescence analysis [1–6]. The rapid development of optical communication system has led to the search for more sufficient compounds for the processing of optical signals. ADP is an excellent inorganic NLO material and has a considerable interest amongst several research workers because of its wide frequency, high efficiency of frequency conversion, higher damage threshold against power laser with the aim of improving the second harmonic generation (SHG) efficiency of ADP researchers have attempted to modify ADP crystals either by doping different type of impurities or by altering the growth conditions [7–14]. The addition of some transition metal ion is generally influenced the growth kinetics, habit modification and large single crystals [15]. The growth promotion effect (GPE) of ADP observed in the presence of organic additive [16–26] as well as inorganic additives [27–29]. Although a large number of studies illustrate the effect of dopant have been carried out, no symmetric study on the crystalline perfection in the presence of dopants at different levels, which influence the physical properties an ADP crystals has been reported. Crystalline perfection has a strong influences on the efficiency of the physical properties [30].

The Hg doped and undoped nanocrystalline TiO_2 film on the indium tin oxide (ITO) glass substrate surface and polycrystalline powder were prepared by sol-gel dip coating technique [31]. This study shows that the powder of TiO_2 doped with 5% Hg in room temperature was only composed of the anatase phase. Whereas, in the undoped powder exhibits an amorphous phase were present. Mercury doping in the investigation range has negligible effect on both crystal structure and transport properties as well as Raman spectra of magnesium diboride regime is studied by Elsabawy and Kandyel [32]. The effect of mercury doping on the superconductivity, crystal structure and electronic structure have been investigated in Hg doped $BaPb_{0.75-x}Hg_xBi_{0.25}O_3$ (BPHBO) by magnetic measurements and XRD [33]. This reveals Hg substitution to have considerable influence in the lattice parameters. The effectiveness of ground granulated blast furnace slag (GGBFS) added chemically bonded phosphate ceramic matrix on the stabilization/solidification (S/S) of mercury chloride and simulated mercury-bearing light bulbs (SMLB) [34]. This study shows that the maximum compressive strength was achieved. When 15 and 10% ground GGBFS was added for $HgCl_2$ doped and SMLB doped chemically bonded phosphate ceramic (CBPC) matrixes. The presence of

*Corresponding author: ***Dr. S. Senthilkumar,*** *Chemistry Wing (DDE), Annamalai University, Annamalainagar 608 002, India*

Hg^{2+} ions in the $CaWO_4$ lattice influence the luminescence by pure $CaWO_4$ drastically, due to efficient energy transfer from host lattice groups of the emitting center [35].

The solidification behavior of mercury doped alkali activated slag (AAS) matrix is reported. Further low concentration of Hg^{2+} ion can be effectively immobilized in the AAS matrix [36]. In the present work, the effect of mercury at various concentrations of 1, 5 and 10 mol% doped with ADP has been studied by using FT-IR, UV-Vis, SEM-EDS, TGA-DTA and SHG measurements.

2. MATERIALS AND METHODS

Synthesis and crystal growth

Ammonium dihydrogen phosphate (ADP) (E. Merck) was purified by repeated crystallization. The Hg(II) in the form of mercury chloride was used for the precipitation of single crystals were grown by slow evaporation of solution growth technique (SEST). Three different concentrations of dopant Hg(II) *viz.*, 1, 5 and 10 mol% were used. The prepared solution was filtered with micro filter. Crystallization took place within 15–20 days and crystals were harvested when they attained an optimal size and shape. Photographs of the grown doped and undoped crystals are shown in Fig. 1.

Characterization technique

The Fourier transform infrared (FT-IR) spectra were recorded using Avatar 330 FT-IR by the KBr pellet technique. The UV-Vis absorption spectra were recorded by using a Hitachi UV-Vis spectrophotometer in the spectral range 200–800 nm for all the samples. The powder X-ray diffraction was performed by using a Philips Xpert Pro Triple-axis X-ray diffractometer at room temperature using a wavelength of 1.54 Å and a step size of 0.008°. The samples were examined with Cu-K_α radiation in a 2θ range of 10 to 70°. The XRD data were analyzed by the Rietveld method with RIETAN-2000 [37].

Morphologies of the samples and the presence of dopants in the specimens were observed by using JEOL JSM 5610 LV scanning electron microscope with a resolution of 3.0 nm, an accelerating voltage of 20 kV and a maximum magnification of 300,000 times. In order to know the thermal stability of the grown crystals thermogravimetric analysis (TGA) and differential thermal analysis (DTA) were performed using Perkin Elmer Diamond TG-DTA thermal analyzer at heating rate 20 °C min^{-1} ranging from 0–800 °C at inert nitrogen atmosphere. The SHG efficiency of the specimens was measured by the Kurtz powder method [38].

3.RESULTS AND DISCUSSION

FT-IR spectral analysis

The infrared spectral analysis was carried out to understand the chemical bonding and it provides useful information regarding the molecular structure of the compound. FT-IR spectrum was taken from the powdered sample of various concentrations of Hg doped ADP crystals in the wavelength range 400–4000 cm^{-1} is shown in Fig. 2. FT-IR spectra of pure ADP the O–H stretching vibration of water assigned at 3126 cm^{-1}, P–O–H stretching at 1103 cm^{-1}, N–H stretching of ammonia at 2852 cm^{-1} and PO_4 vibrations give their peaks at 549.1 and 452 cm^{-1}. The FT-IR spectra of mercury (1, 5 and 10 mol%) doped ADP crystals showed that the peak position have been moved from higher to lower wave number due to the presence of Hg into ADP. For example, the PO_4 vibration of the parent is shifted from 452 to 425 cm^{-1}, which was confirmed the presence of mercury on the lattice of ADP crystals. Table 1 shows the vibrational frequencies corresponding to band assignments.

Table 1 Vibrational frequencies (cm^{-1}) for pure ADP and Hg doped ADP crystals.

Pure ADP	Hg doped ADP 1 mol%	5 mol%	10 mol%	Assignment
3126	3112	3133	3112	O–H stretching
2852	2860	2849	2854	N–H stretching NH_4
1402	1404	1402	1403	Bend stretching of NH_4
1292	1288	1292	1289	Combination band of stretching
1103	1100	1103	1101	P–O–H stretching
549	547	545	548	PO_4 stretching
452	449	447	425	PO_4 stretching

Table 2 Lattice parameter values for pure ADP and Hg doped crystals.

Crystal	$a=b$ (Å)	c (Å)	V (Å^3)	System
Pure ADP	7.502	7.566	428.6	Tetragonal
ADP + 1 mol% Hg	7.530	7.550	430.0	Tetragonal
ADP + 5 mol% Hg	7.486	7.539	420.0	Tetragonal
ADP + 10 mol% Hg	7.490	7.530	425.0	Tetragonal

Table 3 SHG output.

System	$I_{2\omega}$ (mV)
Pure ADP	11.6
ADP + 1 mol% Hg	10.4
ADP + 5 mol% Hg	18.0
ADP + 10 mol% Hg	15.0

UV-Vis absorption spectra

The optical absorption spectrum of the pure and doped ADP crystals are shown in Fig. 3. All the crystals have sufficient transmission in the entire visible region and the UV cutoff wavelength is found to be at 400 nm. The low absorption in the entire visible region confirms the suitability for fabrication of nonlinear or optoelectronic application devices. Using the formula $E_g = 1240\ (hc)/\lambda$ (nm), the band gap is calculated to be 5.8, 5.6 and 4.15 eV (Fig. 4), respectively.

Powder X-ray diffraction

Powder X-ray diffraction (XRD) is useful to determine the crystalline and the purity of growing crystals were grown. Fig. 5 shows X-ray powder diffraction patterns of pure ADP and those of the materials grown with Hg solution at 1, 5 and

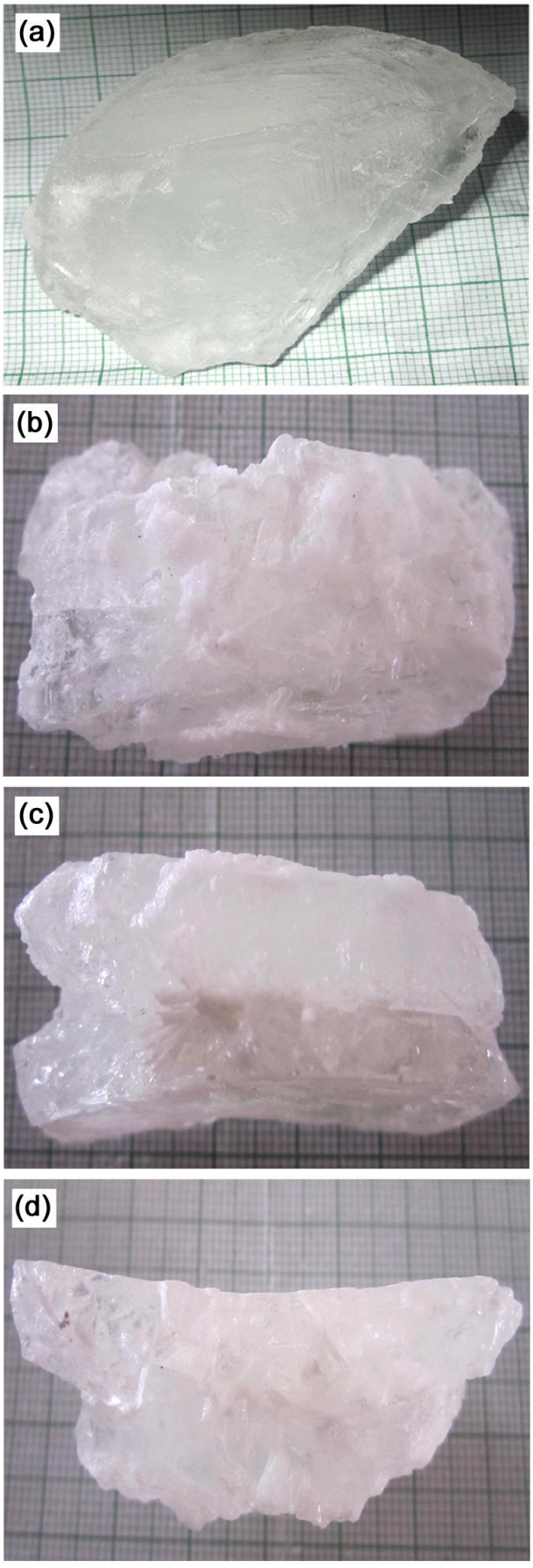

Fig. 1. Photographs of ADP crystals: (a) pure, (b) 1 mol% Hg doped, (c) 5 mol% Hg doped and (d) 10 mol% Hg doped.

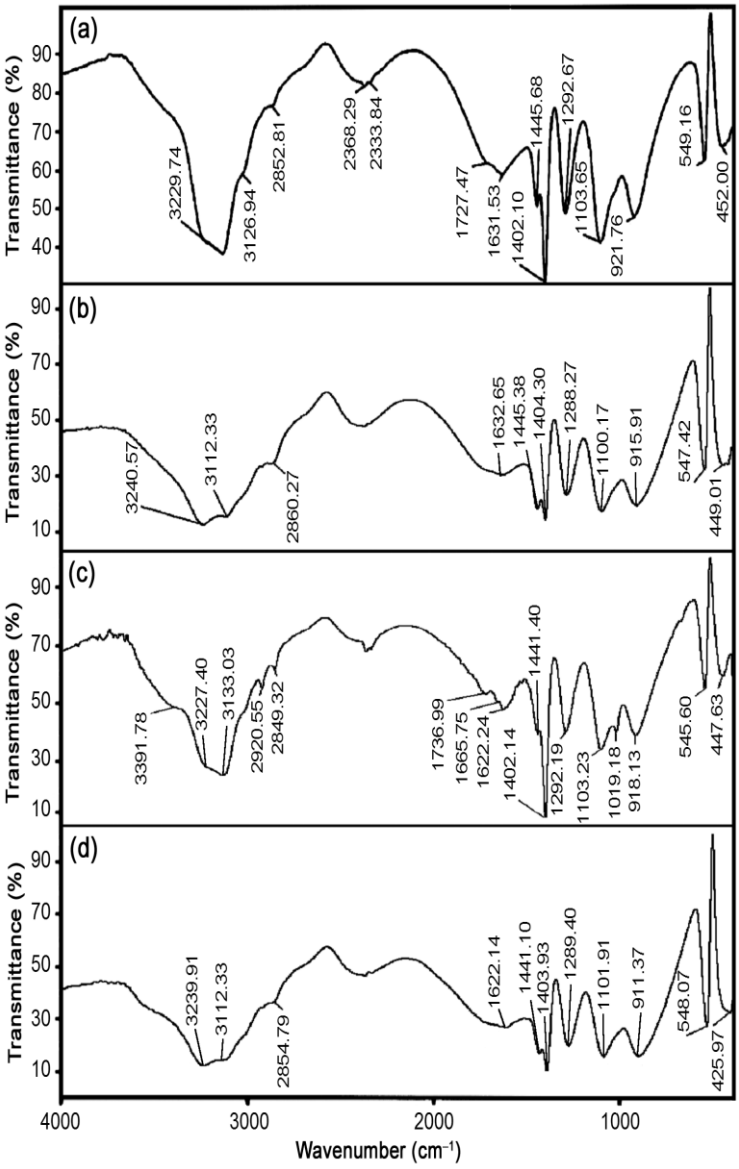

Fig. 2. FT-IR spectra of ADP crystals: (a) pure, (b) 1 mol% Hg doped, (c) 5 mol% Hg doped and (d) 10 mol% Hg doped.

10 mol%. Well defined Bragg peaks are obtained at specific 2θ angles indicating that crystals are ordered. The '*d*' spacing and *h*, *k*, *l* values for prominent peaks in the spectrum were identified and compared with International Centre for Diffraction Data (ICDD). This suggests that the crystals retain almost the single phase structure without detectable impurity. The general observation in that the relative intensities have been reduced and slight shift in the peak position is observed as a result of doping. The cell parameters have been determined from the single crystal X-ray diffraction analyses of pure and doped ADP crystals exhibit very slight variation in unit cell parameters on doping of different concentration of Hg (Table 2). The crystallite sizes (*t*) are calculated using the Scherrer equation [39]

$$t = \frac{K\lambda}{(\beta \cos\theta)}$$

Where *K* is Scherrer constant; λ is the wavelength of X-ray, θ is the peak position measured in radian and β is the integral breadth of reflections located at 2θ.

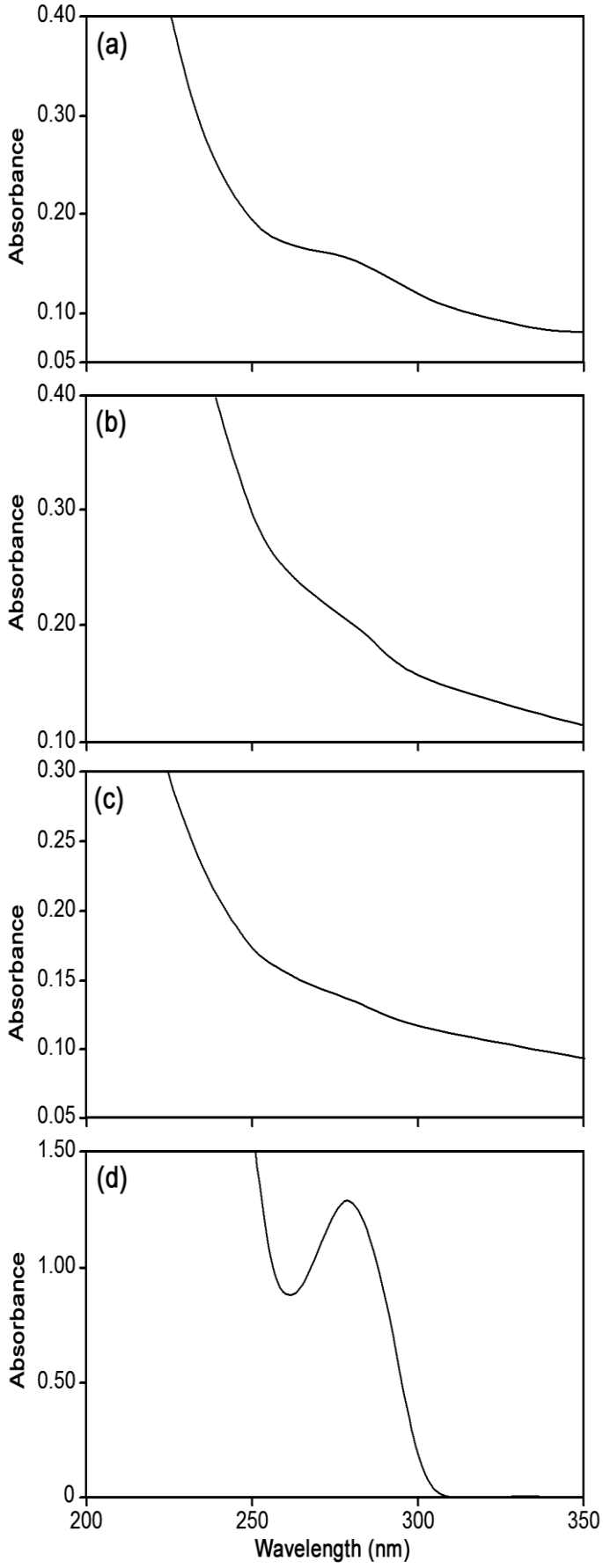

Fig. 3. UV-Vis spectra of ADP crystals: (a) pure, (b) 1 mol% Hg doped, (c) 5 mol% Hg doped and (d) 10 mol% Hg doped.

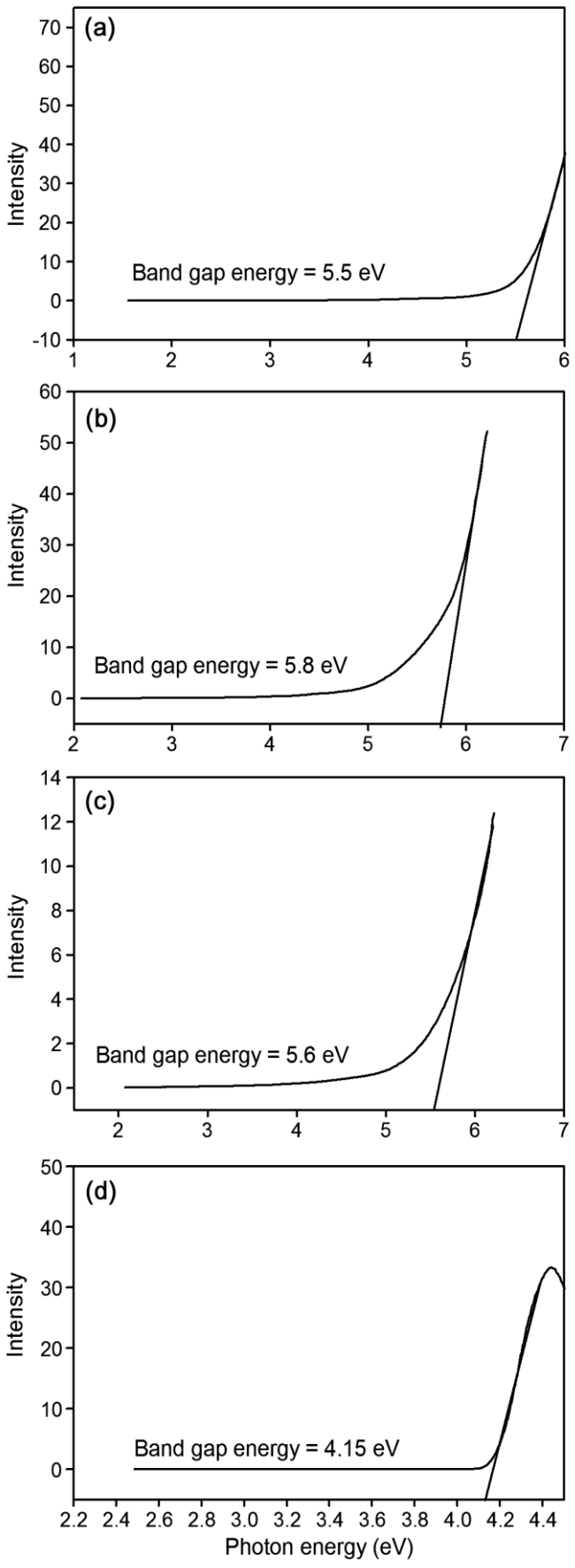

Fig. 4. Band gap energy of ADP crystals: (a) pure, (b) 1 mol% Hg doped, (c) 5 mol% Hg doped and (d) 10 mol% Hg doped.

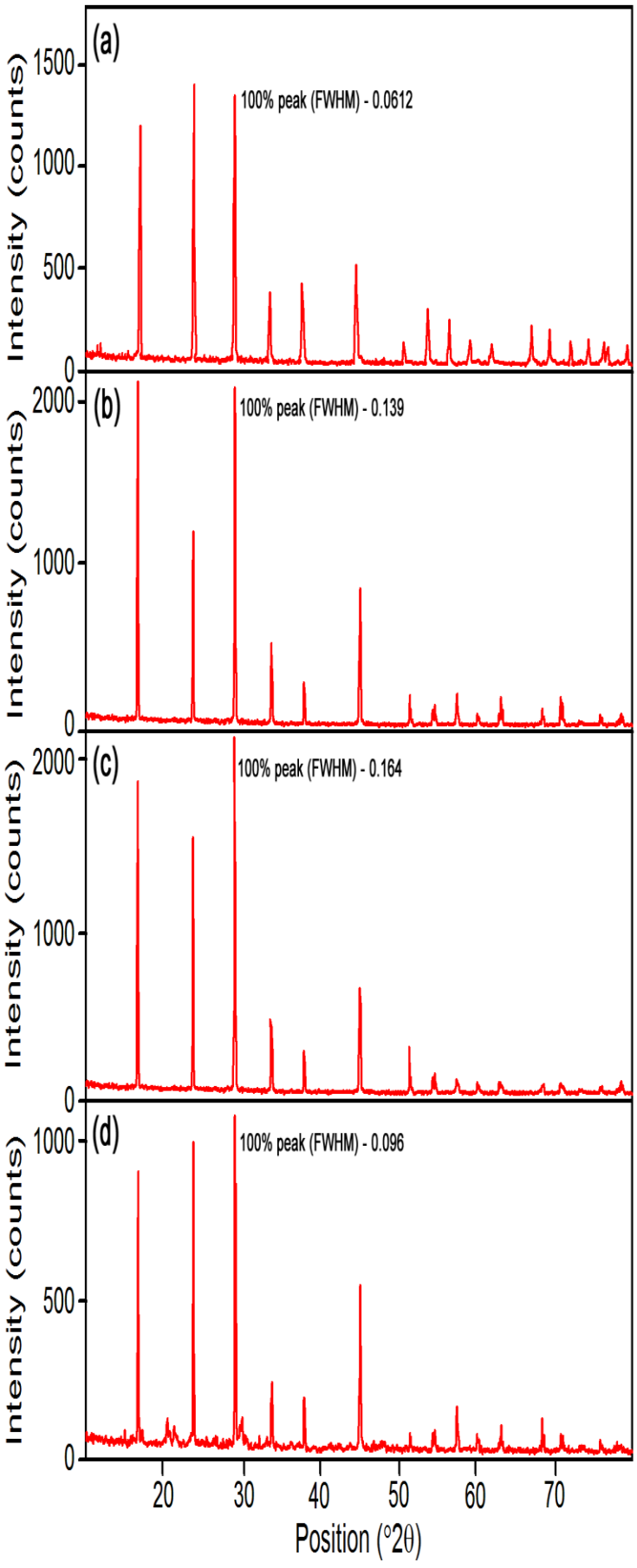

Fig. 5. XRD patterns of ADP crystals: (a) pure, (b) 1 mol% Hg doped, (c) 5 mol% Hg doped and (d) 10 mol% Hg doped.

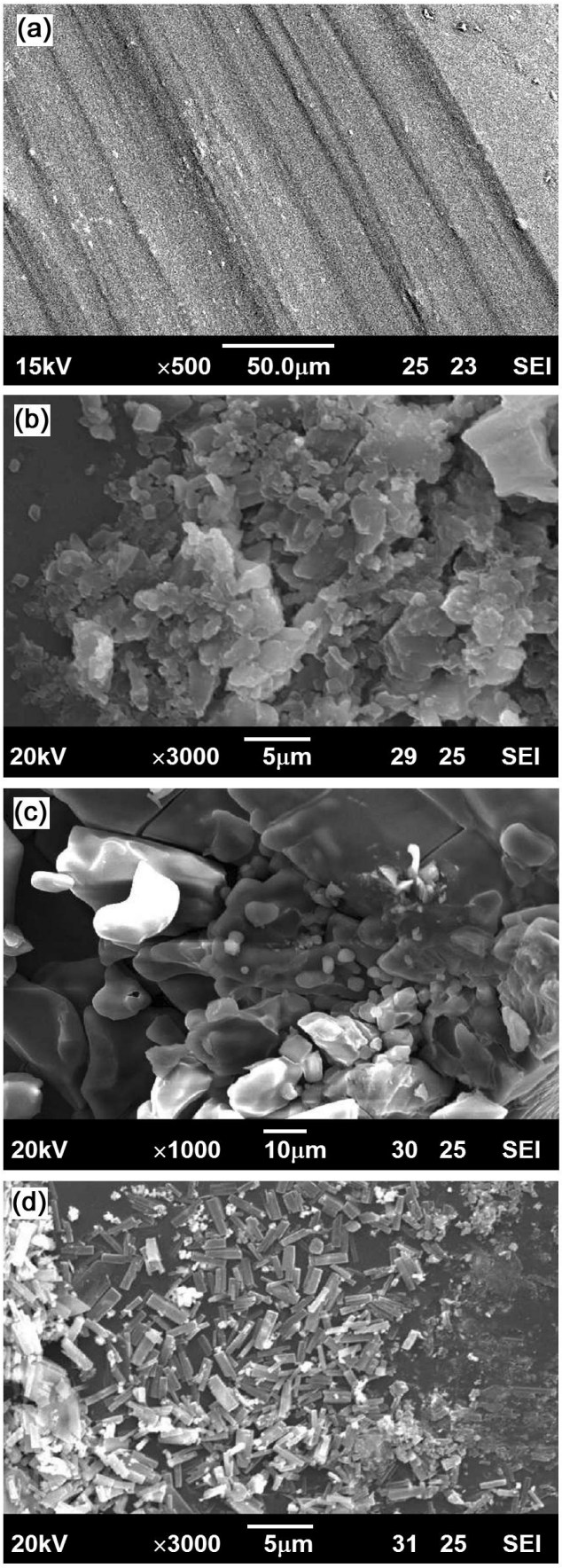

Fig. 6. SEM images of ADP crystals: (a) pure, (b) 1 mol% Hg doped, (c) 5 mol% Hg doped and (d) 10 mol% Hg doped

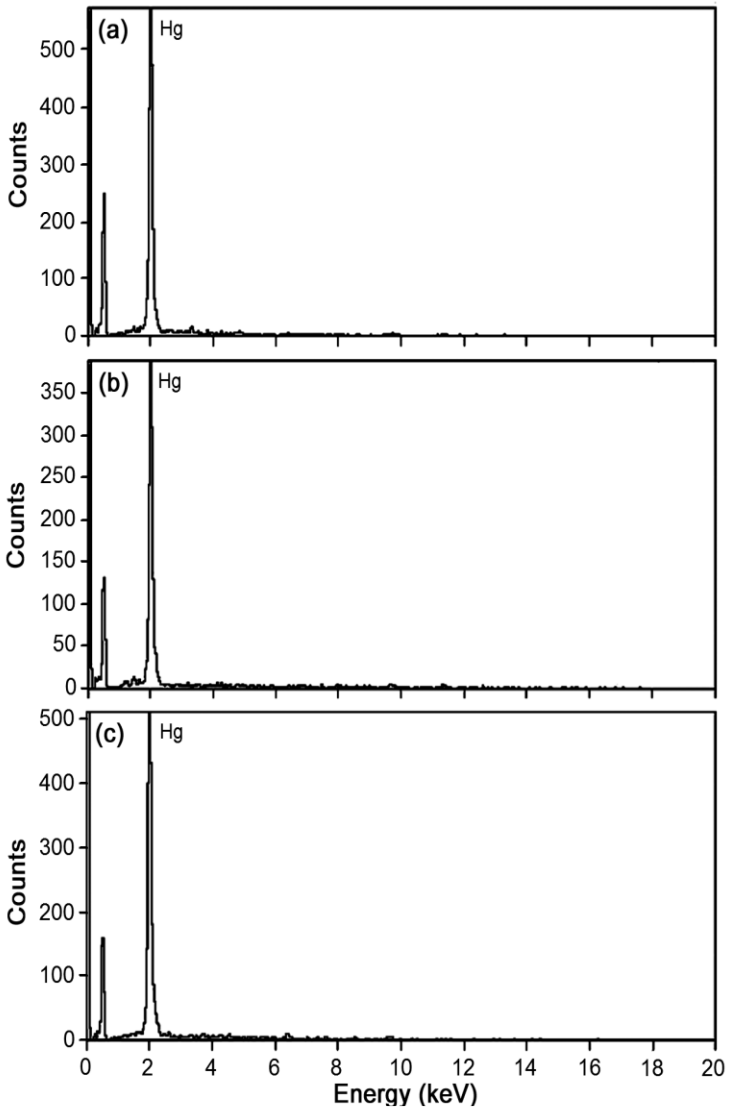

Fig. 7. EDS spectrum of ADP crystals: (a) pure, (b) 1 mol% Hg doped, (c) 5 mol% Hg doped and (d) 10 mol% Hg doped.

SEM-EDS analysis

Scanning electron microscope study gives information about the surface nature and its suitability for device fabrication. It is also used to check the presence of imperfections. It has been reported that the effectiveness of different impurities in changing the surface morphology is different [19]. At low concentrations of dopant the effects are reflected by changes in configuration of growing structures [19]. The SEM photographs are given in Fig. 6. SEM photographs of pure ADP show a layered structure, mostly defect free. In the presence of 1 mol% of Hg in the growth medium, the SEM photograph of ADP crystals shows a cauliflower morphology and in 5 mol% Hg of grown crystals shows dentric structure on the surface. High concentration (10 mol%) results the segregation of dopants at the someplace of the crystals. The incorporation of Hg into the crystalline matrix was confirmed by EDS performed on ADP (Fig. 7). It appears that the accomadating capability of the host crystal is limited and only a small quantity is incorporated into the ADP crystals. Further analyses the surface at different sites indicates that the incorporation is non-uniform over the surface, connected with absorption mechanism. EDS spectra reveal that the concentration of dopant increases with increases in the aqueous growth medium.

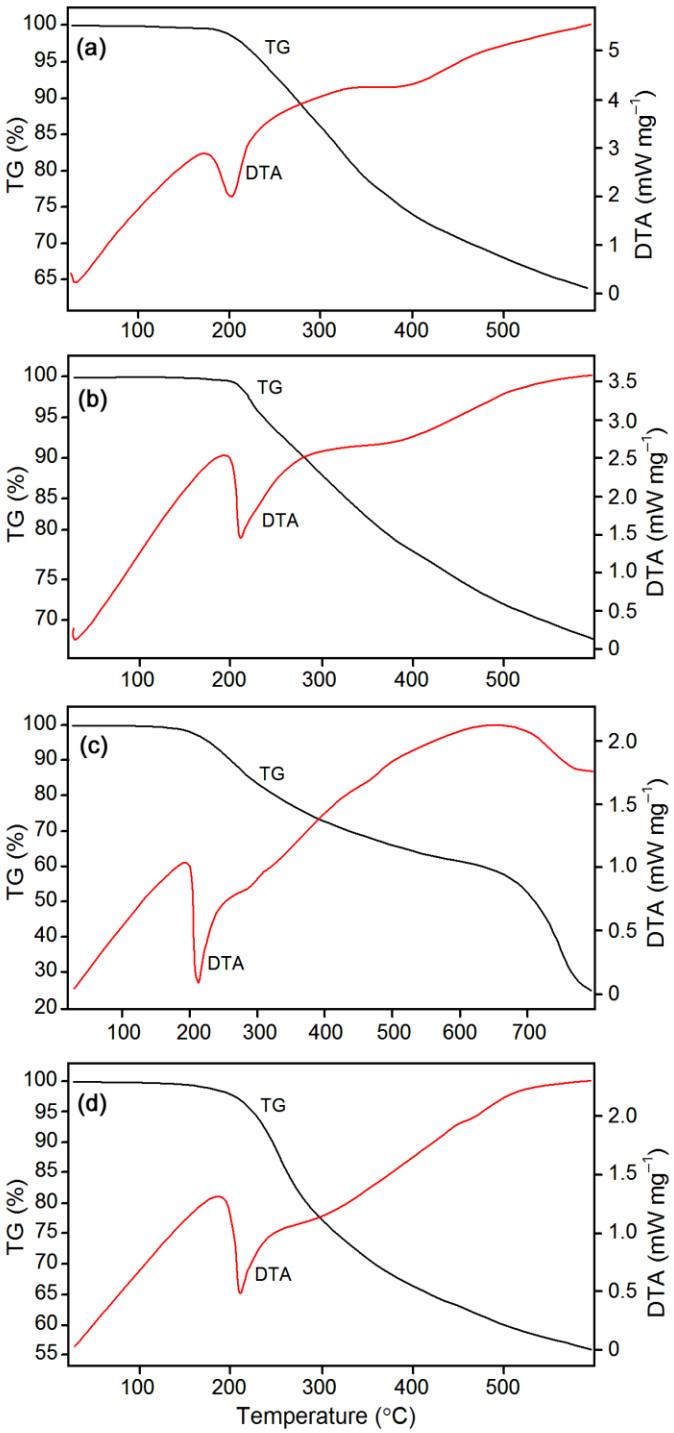

Fig. 8. TG-DTA curves of ADP crystals: (a) pure, (b) 1 mol% Hg doped, (c) 5 mol% Hg doped and (d) 10 mol% Hg doped.

TGA-DTA analysis

Thermogravimetric and differential thermal analysis give the information about phase transition, water of crystallization and different stages of decomposition of the crystal system. The thermal stability of pure and doped ADP at 1, 5 and 10 mol% of Hg in identified by the TGA and DTA studies are shown in Fig. 8. The samples are analyzed between the

temperature 0–800 °C at the heating rate 20 °C min^{-1} in the protected nitrogen atmosphere. The thermal analysis shows that there is no physically adsorbed water in the molecular structure of crystals grown from doped solution. Studies reveal the purity of the materials. The sharpness of the endothermic peak can be attributed to the good degree of crystallinity and purity of the material [40]. Significant variation is not observed. Absence of decomposition up to the melting point ensures the suitability of the material for the application.

SHG analysis

The most widely used techniques for confirming the SHG efficiency of NLO materials to identify the materials with non-centrosymmetric crystal structure in the Kurtz powder technique [38]. A Q-switched Nd:YAG laser beam of wavelength 1064 nm was used with an input power at 4.9 mJ and pulse width 10 ns with a repetition rate of 10 Hz.

The SHG efficiency of pure and Hg doped crystals was confirmed by output green radiation from single crystals during the SHG measurements. The measurement of relative SHG efficiency of undoped and doped crystals was done and show the nonlinear dependence of SHG output on the doping concentration. The SHG output increases with doping concentration of 1 and 5 mol% and then decreased for 10 mol% Hg. The SHG efficiencies with respect to ADP are given in Table 3. These results indicate the strong correlation which in turn depends on dopant concentration. In recent studies, a direct effect of crystalline perfection on SHG efficiency ZTS and ADP crystals has been observed [38,41]. At higher concentration, the size of the dopant is large, so SHG efficiency decrease due to deterioration of crystalline perfection as observed in ADP crystals [42]. In the present investigation also at higher concentration the SHG efficiency was reduced.

4. CONCLUSIONS

The influence of doping of Hg(II) at various concentrations (1, 5 and 10 mol%) on ADP crystal has been studied. Close observation of FT-IR and XRD profile of doped and undoped samples reveal some minor structural variations. These indicate that the crystal undergoes considerable lattice stress as a result of doping. The optical transparency is not destroyed by doping and no decomposition up to the melting point are observed by thermogravimetric analysis. SEM analysis reveals the effectiveness of different morphology and EDS confirm the presence of Hg in the doped specimen. The low concentration of dopant at 1 and 5 mol% appreciably improve the SHG efficiency because of favorable molecular alignment improving the nonlinearity. The higher the concentration, the SHG efficiency, decreasing because of the deterioration of crystalline perfection.

5.REFERENCES

[1] R. Kripal, S. Shukla, P. Dwivedi, Physica B 407 (2012) 656–663.

[2] P. Rajesh, K. Boopathi, P. Ramasamy, J. Crys. Growth 318 (2011) 751–756.

[3] K. Srinivasan, A. Cantoni, G. Bocelli, Cryst. Res. Technol. 45 (2010) 737–746.

[4] R. Ananda Kumari, Ind. J. Pure Appl. Phys. 47 (2009) 369–371.

[5] Y. Asakuma, Q. Li, H.M. Ang, M. Tade, K. Maeda, K. Fukui, Appl. Surf. Sci. 254 (2008) 4524–4530.

[6] X. Ren, D. Xu, D. Xue, J. Crys. Growth 310 (2008) 2005–2009.

[7] K.D. Parikh, D.J. Dave, B.B. Parekh, M.J Joshi, Bull. Mater. Sci. 30 (2007) 105–112.

[8] K.D. Parikh, D.J. Dave, B.B. Parekh, M.J. Joshi, Cryst. Res. Technol. 45 (2010) 603–610.

[9] N. Vijayan, S. Rajasekaran, G. Bhagavannarayana, R. Ramesh Babu, R. Gopalakrishnan, M. Palanichamy, P. Ramasamy, Cryst. Growth Des. 6 (2006) 2441–2445.

[10] P.V. Dhanaraj, N.P. Rajesh, P. Ramasamy, M. Jeyaprakasan, C.K. Mahadevan, G. Bhagavannarayana, J. Cryst. Res. Technol. 44 (2009) 54–60.

[11] P. Praveen Kumar, V. Manivannan, P. Sagayaraj, J. Madhavan, Bull. Mater. Sci. 32 (2009) 431–435.

[12] B. Suresh Kumar, K. Rajendra Babu, Indian J. Pure Appl. Phys. 46 (2008) 123–126.

[13] A. Rahman, J. Podder, Int. J. Optics 2010 (2010) 1–5.

[14] C. Sekar, R. Parimaladevi, J. Optoelectron. Biomed. Mater. 1 (2009) 215–225.

[15] K. Sangwal, E. Meilniczek-Brzoska, J. Cryst. Growth 267 (2004) 662–675.

[16] C.S. Strom, L.J.P. Vogels, M.A. Verheijen, J. Cryst. Growth 155 (1995) 144–155.

[17] S.P. Meenakshisundaram, S. Parthiban, N. Sarathi, R. Kalavathy, G. Bhagavannarayana, J. Cryst. Growth 293 (2006) 376–381.

[18] G. Bhagavannarayana, S. Parthiban, S.P. Meenakshisundarm, J. Appl. Crystallogr. 39 (2006) 784–790 .

[19] K. Sangwal, Prog. Cryst. Growth Charact. 32 (1996) 3–43.

[20] G. Blisnakov, E. Kirkova, Z. Phys. Chem. 206 (1957) 271–280.

[21] E. Kirkova, R. Nikolaeva, Krist. Tech. 6 (1961) 741–746.

[22] R. Kern, R. Dassonville, J. Cryst. Growth 116 (1992) 191–203.

[23] M.L. Barsukova, V.A. Kuznetsov, T.M. Okhrimenko, V.S. Naumov, O.V. Kachalov, A.Y. Klimova, M.I. Kolybaeva, V.I. Salo, Kristallografiya 37 (1992) 1003–1010.

[24] T.M. Okhrimenko, S.T. Kozhoeva, V.A. Kuznetsov, A.Y. Klimova, M.L. Barsukova, Kristallografiya 37 (1992) 1309–1314.

[25] S.P. Kuzmin, V.A. Kuznetsov, T.M. Okhrimenko, S. Bagdasarov, Kristallografiya 39 (1994) 914–917.

[26] V.A. Kuznetsov, T.M. Okhrimenko, S. Bagdasarov, Kristallografiya 41 (1996) 557–562.

[27] V.A. Kuznetsov, T.M. Okhrimenko, M. Rak, SPIE Proc. 3178 (1997) 100–107.

[28] G. Li, L. Xue, G. Su, Z. Li, X. Zhuang, H. Ha, Cryst. Res. Technol. 40 (2005) 867–870.

[29] J. Podder, S. Ramalingom, S. Narayanakalkura, Cryst. Res. Technol. 36 (2001) 549–556.

[30] K. Shantha, S. Philip, K.B.R. Varma, Mater. Chem. Phys. 48 (1997) 48–51.

[31] R. Mechiakh, N. Ben Sedrine, R. Chtourou, Appl. Surf. Sci. 257 (2011) 9103–9109.
[32] K.M. Elsabawy, E.E. Kandyel, Mater. Chem. Phys. 103 (2007) 211–215.
[33] Y. Zhang, Y.L. Chen, C.H. Cheng, Y.J. Cui, Y. Zhao, J. Phys. Chem. Solids 72 (2011) 597–600.
[34] Z. Liu, G. Qian, J. Zhou, C. Li, Y. Xu, Z. Qin, J. Hazard. Mater. 157 (2008) 146–153.
[35] G. Blasse, J. Solid State Chem. 13 (1975) 339–344.
[36] G. Qian, D.D. Sun, J.H. Tay, Cement Concrete Res. 33 (2003) 1251–1256.
[37] G. Bhagavannarayana, S. Parthiban, C. Chandrasekaran, S. Meenakshisundaram, CrystEngComm 11 (2009) 1635–1641.
[38] S.K. Kurtz, T.T. Perry, J. Appl. Phys. 39 (1968) 3798–3813.
[39] A.L. Patterson, Phys. Rev. 56 (1939) 978–982.
[40] S.H. Hameed, G. Ravi, R. Dhanasekaran, P. Ramasamy, J. Cryst. Growth 212 (2000) 227–232.
[41] G. Bhagavannarayana, S.K. Kushwaha, J. Appl. Crystallogr. 43 (2010) 154–162.
[42] G.Bhagavannarayana, S. Parthiban, S. Meenakshisundaram, Cryst. Growth Des. 8 (2008) 446–451.

*****